

## **The continuous combustion of glycerol in a fluidised bed**

**I.A. Gibson<sup>a</sup>, C.J. Slim<sup>a</sup>, Yaoyao Zheng<sup>b</sup>, S.A. Scott<sup>b</sup>, J.F. Davidson<sup>a</sup>, <sup>a</sup>A.N. Hayhurst<sup>a\*</sup>**

*<sup>a</sup>Department of Chemical Engineering and Biotechnology, University of Cambridge, Philippa Fawcett Drive, Cambridge CB3 0AS, UK.*

*<sup>b</sup>Department of Engineering, University of Cambridge, Trumpington Street, Cambridge CB2 1PZ, UK.*

### ***Keywords:***

Fluidised bed combustion

Combustion of liquids

Combustion of glycerol

Mixing in fluidised beds

**n.b. Figs 2 & 3 are the only Figs needing colour**

**\* Corresponding author**

**E-mail address: [anh1000@cam.ac.uk](mailto:anh1000@cam.ac.uk)**

## Abstract

It is difficult to burn a liquid fuel inside a fluidised bed. For the first time, liquid glycerol has been burned, when continuously injected into the bottom of an electrically heated bed of alumina particles (sieved to 355 – 425  $\mu\text{m}$ ), fluidised by air. The temperature in the bed was held at 700, 800 or 900°C; usually  $(U/U_{mf})$  was 2.5. The bed's depth was varied, as also were  $(U/U_{mf})$  and the ratio of fuel to air supplied to the bed. Measurements were made of the concentrations of  $\text{CH}_4$ ,  $\text{O}_2$ ,  $\text{CO}$  and  $\text{CO}_2$ , and also of the temperature, in the freeboard well above the bed. On entering the bed, the liquid glycerol, rapidly formed bubbles of vapour, which quickly decomposed thermally, yielding mostly  $\text{CO}$  and  $\text{H}_2$ . These gases then mixed with the other gases in the bed. It appears that the diffusive  $\text{H}_2$  mainly burns between the fluidised particles. With the bed at 700 – 900°C, no  $\text{CO}$  was detected far downstream of the bed, provided the equivalence ratio,  $\theta$ , was below 0.7, *i.e.* with more than 43 % excess air. Under these fuel-lean conditions, all the carbon in the glycerol was oxidised to  $\text{CO}_2$ . However, in a more fuel-rich situation, with  $\theta > 0.7$ ,  $\text{CO}$  was detected well above the bed, particularly with a deeper bed, at a lower temperature and operating more fuel-rich. Thus, with the bed at 900°C,  $\text{CO}$  was mostly oxidised inside the bed, but occasionally some  $\text{CO}$  burned on top of the bed. When a fuel-rich bed was below  $\approx 850^\circ\text{C}$ , not all the  $\text{CO}$  burned in the bed. Achieving complete combustion inside a fluidised bed is partly a problem of mixing the products of glycerol's thermal decomposition with the fluidising air, which on entry exists mainly in bubbles. Consequently, increasing  $(U/U_{mf})$  promoted both mixing and combustion in a bed. In addition, in-bed combustion requires the bed to be sufficiently deep, hotter than  $\approx 850^\circ\text{C}$  and  $\theta$  to be less than a critical value. The effects of other variables are discussed.

## Nomenclature

$d_b$	diameter of a bubble, m
$g$	acceleration due to gravity, $9.806 \text{ m s}^{-2}$
$G$	volumetric flowrate of glycerol vapour into a bed, $\text{ml s}^{-1}$
$T_{bed}$	temperature of a bed, K or $^{\circ}\text{C}$
$U$	superficial velocity of fluidising air through a hot bed, $\text{m s}^{-1}$
$U_{mf}$	value of $U$ at incipient fluidisation, $\text{m s}^{-1}$
$U_{rise}$	rise velocity of a bubble, $\text{m s}^{-1}$
$V_b$	volume of a bubble, $\text{m}^3$
$x_i$	mole fraction of species $i$ in the gas phase
$\varepsilon_{mf}$	voidage in a bed at minimum fluidisation
$\theta$	equivalence ratio = (fuel supplied / fuel for a stoichiometric mix with the $\text{O}_2$ supplied)
$\theta_{crit}$	minimal value of $\theta$ for producing CO in the off-gases
$\psi$	$x_{\text{CO}}/(x_{\text{CO}} + x_{\text{CO}_2})$

### 1. Introduction

Biodiesel is a good, renewable motor fuel; blended with Diesel fuel it performs well in a conventional engine. Also, pure biodiesel can be used in purpose-built engines. The biodiesel market has grown steadily, so huge volumes are now consumed, particularly in the Americas [1]. Glycerol ( $\text{CH}_2\text{OH}.\text{CHOH}.\text{CH}_2\text{OH}$ ) is produced as the major waste product in the transesterification of natural oils to produce biodiesel. In fact, up to 10 wt.% of the reaction products can be glycerol [2], so, as the biodiesel market grows, there are increasing concerns as to how to utilise all the waste glycerol.

This study investigates the viability of burning waste glycerol continuously in a fluidised bed. This would avoid the difficulties of atomising such a viscous liquid for a conventional burner. Menon *et al.* [3] found that the batchwise combustion of glycerol in a hot, fluidised bed of alumina particles is sometimes difficult below  $800^{\circ}\text{C}$ . This was because the glycerol entered the electrically heated fluidised bed as fairly large bubbles of vapour, which did not mix rapidly with the fluidising air, located in quite separate bubbles. In fact, burning mainly occurred above

the bed. However, it was clear that no soot was produced, if the glycerol was released reasonably deep down a bed [3]. This mirrors the problems experienced by Stubington and Davidson [4], who tried to burn kerosene, a typical liquid fuel, in an electrically heated bed of silica sand, fluidised by air. The kerosene was fed via a tube to the bottom of the fluidised bed. Thus a train of bubbles of hot kerosene vapour rose up through the bed, together with bubbles of fluidising air. However, depending on the precise conditions, much of the fuel burned in the freeboard above the bed, largely because of the difficulty of mixing the fuel's vapour with air, both of which were initially located separately in fairly large bubbles. Thus one challenge of burning a liquid fuel in a fluidised bed is to mix quickly the vapour of the fuel with the fluidising air; as discussed below, this is difficult if each are initially present in large bubbles.

It should be mentioned that Bohon *et al.* [5] have successfully burned glycerol in a high-swirl, prototype burner, coupled to a refractory-lined furnace. Their properly designed burner achieved stable combustion, in spite of some difficulties with autoignition and glycerol's high viscosity. There was particular concern about the variable composition of the glycerol feedstock. Combustion was optimal under fuel-lean conditions ( $0.37 < \theta < 0.44$ ). Here the overall composition is defined by the equivalence ratio:

$$\theta = \frac{\text{Actual ratio of (fuel/air) fed to the bed}}{\text{Ratio of (fuel/air) for a stoichiometric mix}} = \frac{\text{fuel supplied}}{\text{fuel for a stoichiometric mix with the } O_2 \text{ supplied}} \quad (1)$$

Thus  $\theta < 1$  means the mixture is fuel-lean and  $\theta > 1$  signifies the mixture is fuel-rich. A stoichiometric mixture of fuel and oxygen refers to:



Reaction (I) makes it clear that glycerol is an oxygenated fuel with the atomic ratio C/O = 1 per molecule. Thus there is enough oxygen in glycerol to burn all the carbon to CO, assuming that none of the hydrogen is oxidised.

The amounts of formaldehyde and acetaldehyde emitted during the experiments of Bohon *et al.* [5] were low [5] and very similar to those observed when burning propane or a fuel-oil, *i.e.* the combustion of glycerol was fairly rapid, with negligible emissions of hydrocarbons. Fly ash particles appeared in the off-gas and suggested that, if left untreated, the catalyst (used in the transesterification) might cause problems, if waste glycerol were burned in an incinerator [5, 6]. Other concerns [6, 7] about waste glycerol as a fuel include the possibility of emissions of

acrolein, *i.e.* allyl aldehyde,  $\text{CH}_2=\text{CH}\cdot\text{CHO}$ , which is toxic at low concentrations. Steinmetz *et al.* [6] found that the combustion of crude glycerol might emit volatile organic compounds (VOCs) in amounts similar to those from burning natural gas. Gupta & Kumar [8] found that burning glycerol at higher temperatures up to  $\sim 1000^\circ\text{C}$  reduced the production of acrolein very significantly.

## 2. Apparatus

### Figure 1 hereabouts

The bed of solid alumina particles was housed in a stainless steel tube (height 1130 mm, i.d. 78 mm), which was surrounded by electrical heating coils, operated by a PID controller using a K-type thermocouple immersed in the bed. A schematic cross section is shown in Fig. 1. The bed could be heated to slightly above  $1000^\circ\text{C}$ . Fibreglass insulation was packed around the heating coils to reduce losses of heat. Laboratory air was passed through the bed via a square-pitch array of 36 holes (diam. 0.4 mm) in the distributor plate, which had a central inlet tube (i.d. 1.753 mm, o.d. 3.175 mm, stainless steel) feeding liquid glycerol of medicinal purity. The bed contained alumina particles (sieved to be from 355 to 425  $\mu\text{m}$  [9], with a geometric mean of 388  $\mu\text{m}$ ). They were angular with some very sharp points [9]. The flowrate of air to the bed was controlled by a rotameter, for rates up to 48 litres/min, as measured at ambient pressure and temperature. For elevated temperatures, the ideal gas law was used to deduce the air's superficial velocity,  $U$ , *i.e.* the actual volumetric flowrate of air at the temperature of the bed, divided by the bed's cross-sectional area, *i.e.* neglecting the presence of the particles. One source of error arose from the float of the rotameter oscillating at higher flowrates, above  $\sim 30$  litres/min. This made it more difficult to measure very large flowrates of air.

When the flowrate of air through a bed of particles is increased gradually above zero, the particles remain stationary until  $U$  reaches a critical value,  $U_{mf}$ , when all the particles begin to move. This is the onset of fluidisation;  $U_{mf}$  was measured at elevated temperatures in the bed in a separate study [9], where further details can be found. When  $U = U_{mf}$ , the pressure drop across the bed is just sufficient to support the submerged weight of the particles. If  $U > U_{mf}$ , the air in excess of that for minimum fluidisation usually flows as bubbles vertically up through the bed of fluidised particles, which are supported by drag forces, caused by air flowing over the particles.

Thus, when  $U > U_{mf}$ , gas usually passes up a bed as bubbles and also interstitially between fluidised particles. There is exchange of gas between the bubbles and that flowing interstitially. The bubbles do move radially sideways in their ascent and appear to burst on leaving the bed. In this study the ratio of the actual superficial velocity at the bed's temperature,  $U$ , to  $U_{mf}$  was usually 2.5, but was varied, as described below. Such a value is high enough for the temperature in the fluidised bed to be uniform, except of course, very close to the slightly hotter walls.

Medicinal glycerol was fed to the bed, using a peristaltic pump (Watson-Marlow 101U), which regularly squeezed a soft rubber tube, connected to the stainless steel inlet tube feeding glycerol into the hot bed (see Fig. 1). This tube was central and protruded 1 mm into the bed. A wire mesh gauze, shown in Fig. 1, was fastened across the top of the tube to prevent alumina particles falling into and blocking the tube. The peristaltic pump was calibrated by measuring the mass of glycerol delivered in a given time. The flowrate of glycerol was actually varied up to 8.0 g/min. At low flowrates of glycerol, the pump released liquid glycerol into the hot bed in almost discrete pulses. This is described below, but it suggests that glycerol was evaporating rapidly from the tip of the injector, rather than creating a puddle under the wire gauze. This is not surprising, given that the tip of the injector is likely to be hotter than the boiling point (290°C) of glycerol with the bed usually at 700°C or hotter. The result was that bubbles of glycerol vapour rose up the centre of the bed, surrounded by bubbles of fluidising air. Thus the bed operated like a diffusion flame. Bubbles of both air and of glycerol vapour are shown in Fig. 1. Fortunately, during the calibration of the peristaltic pump, it was found that even when the delivery was no longer continuous, the flowrate averaged over a reasonable time was as expected. This meant that provided combustion experiments were run for a few minutes to achieve a steady state, this unsteadiness in the flow of glycerol, discussed below, did not present any problems.

## 2.1 Sampling and analysis of the off-gases

A stainless steel tube (i.d. 3.86 mm, o.d. 6.35 mm, shown in Fig. 1) was used to sample the off-gases from the region above the bed, defined as the freeboard. The open end of the sampling tube was normally positioned 500 mm above the distributor. Thus with a fluidised bed typically ~ 175 mm deep (~ 162 mm, when it was not fluidised), the point of sampling was ~ 325 mm above the top of the bed and ~ 630 mm below the top of the tube housing the bed. Such an arrangement allows time for combustion to occur above the bed and before the point of sampling. A thermocouple was sometimes attached to the sampling tube to measure the

temperature of the sampled gas, as described in more detail below. With the bed at 800°C,  $U_{mf}$  was 0.114 m/s [9], so that with  $U/U_{mf} = 2.5$ ,  $U$  (the velocity in the freeboard) was 0.285 m/s. This indicates that the interval between gas leaving the bed and reaching the sampling probe was  $0.325/0.285 \approx 1.1$  s.

It is important to note that, just above the bed, the freeboard is a vigorously turbulent region, because of the effects of “ghost bubbles” [10], which are bubbles bursting on entering a “splash zone”, when leaving the upper surface of the bed. These ghost bubbles are pockets of gas, which retain their identity on entering the freeboard; they cause “velocity fluctuations of the same order as the mean velocity, which is the fluidising velocity” [10]. This results in localised turbulence, which promotes radial mixing of gas early in the freeboard. This contrasts with mixing within a fluidised bed, where mixing of gas inside bubbles with that percolating between the particles may be relatively slow.

A cover (with holes for the sampling tube and thermocouple to pass through) usually sat on top of the tube housing the hot bed. In this way, any ingress of laboratory air into the sampled gas was prevented. However, this cover was occasionally removed to make visual observations (via a mirror) of the bed’s upper surface. The sampled gas was passed through drying tubes; the first employed a membrane (Nafion), which did most of the drying; the second contained anhydrous calcium chloride, which was daily replaced with fresh desiccant. The dry sample next entered a gas analyser (ABB EL3020, involving: Uras 26, infra-red for CO, CO<sub>2</sub> and CH<sub>4</sub> and Magnos 26, paramagnetic for O<sub>2</sub>). A vacuum pump and a rotameter were used to achieve a constant flowrate of sampled gas (1.0 litre/min, expressed at room temperature and pressure) through the analyser. Gas mixtures of known compositions were used to calibrate the instruments for these four different gases. Checks of the calibrations were made with and without a tube of CaCl<sub>2</sub> in the drying chain; this desiccant did not affect measured concentrations, indicating that drying was mainly done by the membrane. All measurements were recorded continuously at a frequency of 1 Hz on a data logger. Every measurement was checked at least once.

Figure 2 shows the output from a preliminary experiment. It presents the mole fractions (on a dry basis) of three components (O<sub>2</sub>, CO and CO<sub>2</sub>) in the sample; strikingly no methane was ever detected. Each of the five pulses (either as peaks or troughs) represents a continuous combustion run at a particular flowrate of glycerol, when operating with a constant flowrate of air and temperature of 700°C in the bed. The flowrate of glycerol to the bed was increased after

each run, explaining why the depth of the  $O_2$  troughs and the heights of the  $CO_2$  peaks increased with time. Between these peaks and troughs the baseline refers to no glycerol supplied to the bed, *i.e.* the gas analysed was air. Hence, the mole fraction of  $O_2$  was then 0.21, and those of CO and  $CO_2$  were zero.

### Figure 2 hereabouts

There are noticeable oscillations in the readings, particularly at the lower flowrates of glycerol (earlier times on Fig. 2). This was a result of the unsteady delivery from the peristaltic pump, which released low flowrates of glycerol in pulses, rather than as a constant flow. Figure 2 shows that these oscillations became smaller when the flowrate of glycerol was increased and the pump was delivering a more constant flow. The ‘pulses’ were averaged to yield an estimate of the water-free, mole fraction of each gas at the particular conditions for that period. The oscillations in the signals in Fig. 2 make it clear that a measurement of a mole fraction has a larger error in a more fuel-lean situation. The errors in these time-averaged concentrations of CO and  $CO_2$  were  $\sim 3\%$ , but for  $O_2$  the uncertainty was higher at  $\sim 5\%$ .

Most importantly, these time-averaged concentrations of CO,  $CO_2$  and  $O_2$ , as shown in Fig.2, were found not to vary, if the sampling point was moved horizontally and radially off the axis of the freeboard. This indicates good radial mixing of gas above the splash zone and certainly at more than 100 mm above the bed and well below the normal height of sampling. This conclusion was confirmed by measuring the temperature at fixed heights more than 100 mm above the top of the bed whilst burning glycerol. No radial variation in temperature was actually found, except close to the walls of the hot tube housing the bed. As noted above, this good radial mixing was caused by turbulence from ghost bubbles [10] low in the freeboard; such mixing provides the basis for making a coherent set of measurements of the composition and temperature of the gas leaving the freeboard.

It will be seen below that the carbon in the glycerol was completely oxidised to either CO or  $CO_2$ . This is in accord with the above observation of  $CH_4$  never being detected, even when combustion was overall very fuel-rich. Thus it would appear that all the hydrogen in the glycerol fed to the bed was burned to  $H_2O$ . Assuming this to be the case enabled a mass balance to be used to deduce the mole fraction of water in the exit gas and the actual mole fractions of every gas leaving the bed. It was found that the carbon and oxygen balances (comparing atoms before and after burning) were equal to within less than 10 % for most measurements. This provides



reasonable proof that the mass balances hold accurately, as a result of combustion occurring completely somewhere before the point of sampling. Burning could be either inside the bed or as a flat flame on the bed's upper surface or in disengaging bubbles or in the freeboard above the bed. That the mass balances for the elements carbon and oxygen held so well confirmed that the procedures for handling the measurements were appropriate. In particular, it is clear that there were no significant radial variations in the composition and temperature of the off-gases at the height of sampling, as assumed above.

### 3. Results and Discussion

#### 3.1 Visual Observations

Removing the cover from a hot bed burning glycerol revealed the bed's bright, reddish-yellow, upper surface, the brightness and colour depending on the bed's temperature. First, the combustion of glycerol was observed with the bed at 700, 800 or 900°C, with  $U / U_{mf} = 2.5$  and various depths of the bed. The value of  $\theta$  was also varied at 800°C. With beds shallower than 100 mm, deep, quite loud, "popping" noises were heard. Such sounds have been heard before [11 - 14], when fluidising a hot bed of sand with *e.g.* a mixture of propane in air, or alternatively by burning batches of glycerol in a hot bed fluidised with air [3]. These "popping" noises have been ascribed [11 - 14] to bubbles, containing mixtures of a fuel and air, exploding on leaving a bed. Here the loud "pops" were only heard from shallow beds 100 mm deep or less; also, they were quieter at a higher temperature. These brief, sharp "popping" sounds are reminiscent of hydrogen exploding in air. In that case, it would appear that glycerol vapour pyrolyses, yielding hydrogen, before the glycerol is oxidised. The noises are discussed again below, but they do suggest that, with a bed shallower than 100 mm, combustion was at least occurring in disengaging bubbles, igniting and exploding as they left the bed. Also, blue flames, indicating the burning of carbon monoxide [15], were seen above a bed (irrespective of its depth) at 700°C, but not at 800 or 900°C. It thus seems that some burning, particularly of CO, occurred on top of a shallow bed at, and probably below, 700°C.

Others have shown [16 – 18] that CO is produced by pyrolysing glycerol. In fact, in order of abundance, the products of pyrolysing glycerol are mainly CO and H<sub>2</sub>, with some CH<sub>3</sub>CHO, CH<sub>2</sub>CH.CHO (acrolein) and CH<sub>4</sub> present [16 – 18], depending on the temperature. The time for complete pyrolysis at 750°C is 0.1 s [17]. That hydrogen is a significant product of

pyrolysing glycerol, might mean that in a shallow bed, the “popping” sounds are produced by mixtures of hydrogen and oxygen exploding in disengaging bubbles. Otherwise, the absence of explosions above deeper and hotter beds might indicate that hydrogen burned inside a deeper or a hotter bed, as opposed to immediately above such a bed. It should be added that yellow flames, looking like a sooty candle flame and indicating the presence of soot particles, were observed for more fuel-rich burning (with overall  $\theta > 0.83$ ) in shallow beds less than 100 mm deep, but only at 700 or 800°C. This means that low in such a bed there were hot bubbles, rich in glycerol, where the atomic ratio C/O exceeded the critical value of  $\approx 0.5$  [15] for the appearance of soot. This observation suggests that  $\theta$  must have locally been above  $\approx 2.3$ , so a lack of mixing low in such a bed probably resulted in regions sufficiently fuel-rich to produce soot very quickly, but with the soot being slow to burn out subsequently. At 900°C the bed was usually quiet, with no flames, blue or yellow, for  $\theta < 0.83$ . The characteristic, strong smell of acrolein was never detected with the bed at 600°C or hotter. However, a mist was sometimes observed above the bed; this might have been disacryl, a polymer of acrolein, formed in a fuel-rich situation. Otherwise, acrolein is normally oxidised fully. Of course, the mist might be fine particles formed by attrition of the alumina in this fluidised bed. To remain as a mist, the particles would have to be too large to be transported out of the freeboard.

### Figure 3 hereabouts

## 3.2 Effect of Changing Fuel-Air Ratio

The equivalence ratio,  $\theta$ , was found by calculating the mass flowrate of glycerol for a stoichiometric mix (using an atom balance) at the particular conditions. According to Eq. (1), the ratio of the actual mass flowrate of glycerol to the value for a stoichiometric mix yielded the value of  $\theta$ . Figure 3 shows the results of a series of experiments measuring the amounts (on a dry basis) of CO, CO<sub>2</sub> and O<sub>2</sub> in the off-gases, for different  $\theta$ , *i.e.* when different amounts of glycerol were fed to the bed at 700, 800 or 900°C. The fluidised depth of each bed was  $\approx 175$  mm;  $U/U_{mf}$  was always 2.5. No CH<sub>4</sub> was ever detected, presumably because it had all reacted before a sample reached the point of sampling. The error in  $\theta$  was always less than 10 %.

Perhaps the most striking thing about Fig. 3 is that the temperature appears to have little effect on the mole fraction of any of the three species observed, in that the measurements can be superimposed on one curve for each of CO, CO<sub>2</sub> and O<sub>2</sub>. Interestingly, Menon, *et al.* [3]

discussed the existence of a minimal temperature of  $\sim 800^\circ\text{C}$  for combustion of glycerol inside a fluidised bed. Such a threshold temperature is not observed in Fig. 3, but will be discussed below. Figure 3 makes it clear that the same relative amounts of CO and CO<sub>2</sub> were produced regardless of temperature. Thus, in Fig. 3 the value of  $\theta$  characterises the composition of the off-gas. That the temperature is not important indicates that combustion is not controlled by chemical kinetics, but more probably by mixing of the fuel and O<sub>2</sub>, *i.e.* by mass transfer, as suspected above.

Figure 3 is characteristic of combustion in that when the equivalence ratio,  $\theta$ , was increased, the amount of O<sub>2</sub> in the off-gas decreased; also the mole fraction of CO<sub>2</sub> increased with  $\theta$  for  $\theta < \sim 0.7$ . This approximately linear region for the amounts of O<sub>2</sub> and CO<sub>2</sub> from burning fuel-lean mixtures with  $\theta < 0.7$ , covers the region where combustion was complete, *i.e.* no CO was produced. Calculations indicated that all the carbon in the glycerol was then converted to CO<sub>2</sub>. Further increases in equivalence ratio, beyond the critical equivalence ratio,  $\theta_{\text{crit}} \approx 0.7$ , resulted in progressively larger mole fractions of CO and a slightly falling mole fraction for CO<sub>2</sub>. Then, for  $\theta > \theta_{\text{crit}}$ , the mole fraction of O<sub>2</sub> fell to almost zero. It looks as if in the oxygen-rich region, where  $0.7 < \theta < 1$ , mixing of bubbles of glycerol vapour with air from bubbles rising up the fluidised bed was too slow for complete oxidation of the carbon to CO<sub>2</sub>. An equivalence ratio of 0.7 is  $\approx 43\%$  excess air. Checks on the mass balance for the element carbon confirmed that it was always oxidised to either CO or CO<sub>2</sub> for  $\theta < 1.2$ .

Figure 4 expresses some of the results in Fig. 3 in a slightly different way. It shows plots, against  $\theta$ , for all three temperatures, of the fraction of the oxygen (fed to the bed), which reacted before the sampling point. Figure 4 displays the expected trend towards 100 % consumption of O<sub>2</sub>, when the system became more fuel-rich. That not quite all the O<sub>2</sub> was consumed in the richest mixtures might reflect experimental errors, but also the slowness of oxidation for CO, when the concentration of O<sub>2</sub> is low. For  $\theta < 0.7$  a linear plot through the origin can be fitted. Again, changing the bed's temperature did not alter the fraction of the oxygen consumed.

**Figure 4 hereabouts**

### 3.3 General Considerations

Figure 1 shows that glycerol was introduced into a bed at or above  $700^\circ\text{C}$  through an orifice at the tip of the stainless steel feeder, which was hotter than the boiling point of glycerol

(290°C). To investigate what might be happening, it is clear from the above that the glycerol must enter a fluidised bed as a vapour and so enter the bubble phase of the bed. The initial volumes of the first bubbles of glycerol vapour, and also of the fluidising air bubbles, were estimated. This was done using Davidson and Harrison's formula [19] for the volume of a bubble (in  $\text{m}^3$ ), formed by detachment from an orifice, usually on the distributor:

$$V_b = 1.138 G^{6/5} / g^{3/5}. \quad (2)$$

Here  $G$  ( $\text{m}^3 \text{s}^{-1}$ ) is the volumetric flowrate, *e.g.* of glycerol vapour or air, to an orifice in the distributor and  $g$  ( $9.806 \text{ m s}^{-2}$ ) is the acceleration due to gravity. For a bed at 800°C with  $U/U_{mf} = 2.5$  and  $\theta = 0.7$ , the flowrate of glycerol was  $0.06 \text{ g s}^{-1}$ , which produced  $0.058 \text{ litre s}^{-1}$  of vapour at 800°C. Equation (2) thus indicates that the bubbles of glycerol vapour have an initial diameter of  $d_b \approx 17 \text{ mm}$ . Also, they are produced every 0.04 s. This calculation ignores any effect of the wire-mesh covering the orifice in the injector for glycerol. As Fig. 1 shows, the bubbles are most probably spherical caps, for which a wake-fraction of 0.15 is appropriate [20] for the angular particles of alumina [9] fluidised here. In addition, the rise-velocity (with respect to the bed's exterior) of a bubble of diameter,  $d_b$ , can be estimated [20] from:

$$U_{rise} = U - U_{mf} + 0.71 (gd_b)^{1/2}. \quad (3)$$

With  $U_{mf} = 0.114 \text{ m s}^{-1}$  and  $U/U_{mf} = 2.5$ , this gives  $U_{rise} = 0.47 \text{ m s}^{-1}$  for an initial bubble of glycerol vapour with a diameter  $d_b = 17 \text{ mm}$ . Thus for a fluidised bed 175 mm deep, one of these bubbles would have a residence time of  $\approx 0.4 \text{ s}$  within the bed. The gap between successive bubbles of glycerol, when rising up the bed, is  $\sim 19 \text{ mm}$ . Finally, the ratio  $\{U_{mf} / 0.71 \epsilon_{mf} (gd_b)^{1/2}\}$  is  $\approx 0.3$ . This is this ratio of the superficial, interstitial velocity of the gas ( $U_{mf} / \epsilon_{mf}$ ) to the rise velocity of a bubble, relative to the surrounding particles. That it is less than unity indicates [19] that such a bubble is large enough to retain inside it a torus of glycerol vapour, which will not mix readily with the air fluidising the bed. As for the air bubbles, they would be expected to have an initial diameter of  $\approx 11 \text{ mm}$ , *i.e.* they are somewhat smaller than the bubbles of glycerol vapour. That means that the gas confined to the torus inside its bubbles is a little less substantial than for a bubble of glycerol. Even so, one can see the difficulties of mixing the fuel and air inside a bed, with the rate-determining step probably being the transfer of glycerol vapour out of its rising bubbles. These bubbles of fuel and air are represented in Fig. 1.

The above numerical considerations are for  $\theta = 0.7$ . It should be stressed that in Figs 3 and 4, the value of  $\theta$  was varied by supplying the glycerol at a different flow rate. Thus in going from  $\theta = 0.7$  to  $\theta = 1.2$ , the flow rate of glycerol,  $G$ , was simply increased by a factor of  $(1.2/0.7) = 1.7$ , whilst maintaining a constant flow rate of air to the bed. According to Eq. (2), the initial volume of a bubble,  $V_b$ , was consequently increased by a factor of  $1.7^{6/5} = 1.9$ . This means that by using a larger  $\theta$ ,  $V_b$  was also increased, admittedly unintentionally, with the result that larger bubbles were being injected into the bed. Larger bubbles of glycerol lead to poorer mixing of the fluidising air with the products of the thermal decomposition of glycerol. Conversely, a decrease in  $\theta$  ought to have improved mixing inside a bed.

The above considerations suggest that with rather poor mixing at  $\theta \geq 0.7$  there is considerable pyrolysis of glycerol vapour within the bed, before any glycerol vapour reacts with oxygen. The major products of pyrolysing glycerol in steam at 700°C have been shown [16-18] (in order of abundance) to be CO ( $\sim 44\%$ ),  $H_2$  ( $\sim 30\%$ ),  $CH_4$  ( $\sim 12\%$ ),  $CH_3CHO$  ( $\sim 5\%$ ) and acrolein ( $\sim 10\%$ ). Furthermore, with a residence time of *e.g.* 0.1 s, only 15 % of the glycerol decomposed at 650°C, but at 750°C the decomposition was complete [17] by 0.1 s. This means that in most of the experiments of Fig. 3, the glycerol experienced complete thermal decomposition before leaving the bed. The product  $H_2$  has a large diffusivity and, when injected into a bed at or above 500°C and fluidised by air, has been shown [21] to burn low down inside the bed, *i.e.* in the interstices between the fluidised particles. However, hydrocarbons, such as  $CH_4$  and  $C_3H_8$  have only previously been studied [12-14] by first mixing them with air and then fluidising a bed of sand with the mixture. Even then with perfect mixing, they burn with difficulty [12-14]. Of course, given the results in Fig. 3, there is the problem of mixing CO [22] and the other products of pyrolysis with the fluidising air. It is most likely that such mixing is slow enough for them not to burn completely within a bed at 700 – 900°C. That suggests these gases burn [14, 23] either when bubbles leave the bed or as a flat flame on top of the fluidised particles or downstream in the freeboard. This scenario would involve two combustion zones, whereby  $H_2$  burns inside the bed, but the other carbon-containing products of pyrolysis are mainly oxidised above the bed. This hypothesis will now be examined further.

### 3.4 Effects of varying ( $U/U_{mf}$ )

Some experiments will now be described for the same three temperatures (700, 800 and 900°C). The ratio ( $U/U_{mf}$ ) was varied from 1.2 to 4.0 (by altering the flow rate of air to the bed),

with the equivalence ratio,  $\theta$ , held at 0.83, *i.e.* 20 % excess air. Also, the unfluidised depth of the alumina was kept constant at 162 mm; of course, the fluidised depth of the bed varied slightly with  $(U/U_{mf})$ . Figure 5 shows a plot against  $(U/U_{mf})$  of the ratio:

$$\psi = x_{CO} / (x_{CO} + x_{CO_2}). \quad (4)$$

This is the ratio of the mole fraction of CO,  $x_{CO}$ , measured in the off-gas, to the sum of the mole fractions of CO and CO<sub>2</sub>. Thus  $\psi$  can be regarded as a measure of how incompletely CO has been burnt to CO<sub>2</sub>. In Fig. 5, when  $(U/U_{mf})$  tends to unity, a negligible fraction of the air forms bubbles on entering the bed. In the absence of bubbles, the fluidised particles are not at all well-stirred. The glycerol still enters the bed as fairly large bubbles, which mainly bypass the bed. Pyrolysis occurs inside these bubbles and maybe some or possibly all the H<sub>2</sub> burns inside the bed. At the same time, some O<sub>2</sub> will pass from the bed into these bubbles of “fuel”. Consequently, leaving the bed are these bubbles and also the air, which has passed between the particles. There is thus minimal mixing of the air with glycerol either inside bubbles or in the freeboard. Thus  $\psi$  is at its largest in Fig. 5 for  $(U/U_{mf}) \rightarrow 1$ . However, when  $(U/U_{mf})$  is increased to  $\sim 4$ ,  $\psi$  decreases to almost zero. At the largest  $(U/U_{mf})$ , the sizes of the bubbles now of both glycerol and air are at their biggest. Also, the residence times of the gases in the bed are smallest and the bed actually becomes deepest. Even so, the higher velocities of the bubbles promote mixing of fuel and air both in and above the bed. Consequently,  $\psi$  in Fig. 5 decreases, when  $(U/U_{mf})$  increases. Overall, it is clear that  $\psi$  is a useful parameter in that it reflects a lack of mixing of the fuel and air in the system. There is no systematic effect of temperature in Fig. 5, as expected for control by mixing. In fact,  $\psi$  is lowest at 700°C and is usually higher at 800°C. At the highest temperature of 900°C,  $\psi$  is intermediate, probably because CO then burns to a greater extent in the bed or immediately on top of the bed.

### Figure 5 hereabouts

### 3.5 Effects of varying the depth of the bed

This conclusion, that mixing of the decomposition products of glycerol with the fluidising air is an important requirement for combustion inside a fluidised bed, is mirrored by Fig. 6. This is a plot of  $\psi$  against the unfluidised depth of the alumina particles for  $(U/U_{mf})$  and  $\theta$  held constant. When the bed was at its shallowest (25 mm), the residence time of a bubble of glycerol in the bed was  $\sim 0.1$  s. This probably made pyrolysis incomplete

inside the bed at the lowest temperature of 700°C. However, such a shallow bed promoted mixing of the fuel and the air, in what was a considerable and vigorous splash zone immediately above the fluidised particles. That some hydrogen was burning in this region would have encouraged the combustion of any undecomposed glycerol, as well as of its products of pyrolysis, such as CO, hydrocarbons or aldehydes. Consequently,  $\psi$  in Fig. 6 is initially low. At the other extreme of a bed as deep as  $\sim 230$  mm, the residence time of a glycerol bubble in the bed was almost 1 s. Also, the bubbles of air and of decomposing vapour of glycerol, each grew [24] more in a deeper bed by coalescing with one another. The result appears to be that these larger bubbles inhibited the mixing of their contents, as if the air bubbles coalesced with neighbouring air bubbles and not with ones of glycerol. Consequently, because of a greater lack of mixing in deeper beds [19],  $\psi$  in Fig. 6 grows, when the depth of the particles increases. Again, the large  $\psi$  in Fig. 6 are symptomatic of poor mixing of the fuel and fluidising air. The effect of temperature in Fig. 6 is again by no means conspicuous, except that the  $\psi$  measured at 900°C are systematically lower, thereby indicating that more CO burns inside a bed hotter than  $\approx 850^\circ\text{C}$ .

**Figure 6 hereabouts**

### 3.6 Profiles of composition and temperature in the freeboard

The freeboard includes that region just above the top of a bed, where bubbles disengage from the bed and burst into a “splash zone”, where some particles are vigorously ejected upwards. Higher above the bed, there were very few particles in the freeboard; this is where the gases were sampled for *e.g.* Fig. 3. To measure the temperature along the axis of the freeboard, the usual stainless steel sampling probe had a thermocouple (K-type; o.d. 1.0 mm), tied along the length of the tube’s exterior, with the measuring tip tucked  $\sim 20$  mm up inside the bottom of the sampling tube. Such an arrangement shielded the tip of the thermocouple from radiation emitted by the hot walls of the tube housing the bed. Consequently, the temperature measured by the thermocouple arises from that of the gaseous sample, with a radiative contribution from the sampling tube.

**Figure 7 hereabouts**

First, Fig. 7 shows the profile of the temperature measured along the axis above a bed held at  $750^{\circ}\text{C}$  with  $U/U_{mf} = 2.5$ ,  $\theta = 0.83$  and an unfluidised depth of the alumina particles of 149 mm. Also included in Fig. 7 are the measured mole fractions of CO and the sum of those of CO and  $\text{CO}_2$ . The sum ( $x_{\text{CO}} + x_{\text{CO}_2}$ ) initially falls in the splash zone, which appears to extend for  $\sim 50$  mm above the bed. After that, there is a gentle rise in ( $x_{\text{CO}} + x_{\text{CO}_2}$ ), suggesting that some species, like a hydrocarbon, *e.g.*  $\text{CH}_4$ , or an aldehyde or even unburnt glycerol, is being oxidised to CO or  $\text{CO}_2$  well above the bed. The initial fall is possibly associated with a lack of mixing in the splash zone, where bubbles are bursting. By contrast, the mole fraction of CO above the bed was always falling. This demonstrates that not all the CO produced within the bed was burned inside the bed, *i.e.* some CO moved into the freeboard, where it was oxidised. The velocity in the freeboard was  $\sim 0.28 \text{ m s}^{-1}$ , so that the residence time of the gas in the freeboard before travelling 400 mm above the bed to the sampling tube was  $\sim 1.5$  s. Such a time is longer than the rise time of a bubble up the bed of no more than 0.4 s, as demonstrated above. Thus there was plenty of time for CO to burn above the bed before the point of sampling. As for the temperature of the gas, Fig. 7 shows that it rises a little on entering the freeboard. This again might indicate burning in that region. However, the temperature did begin to fall in the freeboard, mainly because the tube housing the bed was not thermally insulated right up to its top. In summary, Fig. 7 confirms that CO and other species were being burned in the freeboard after incomplete oxidation inside the bed at  $750^{\circ}\text{C}$ . The final measured sum of the mole fractions of CO and  $\text{CO}_2$  is close to the value (0.162 on a dry basis) expected for total oxidation of all the carbon to  $\text{CO}_2$ .

### Figure 8 hereabouts

Figure 8 presents measurements for a similar bed, except that it was held at the higher temperature of  $900^{\circ}\text{C}$ , with again  $\theta = 0.83$  (20 % excess air) and the same depth for the bed. The striking feature is that almost no CO was detected in the freeboard for these conditions; sometimes a mole fraction for CO of  $\approx 0.001$  was measured. This indicates that most combustion was occurring inside such a hot bed; this was not the case at  $750^{\circ}\text{C}$ , as seen in Fig. 7. Apart from a slight rise in the splash zone, where the measurements were somewhat noisier, in Fig. 8 the sum ( $x_{\text{CO}} + x_{\text{CO}_2}$ ) is constant above



the bed. Its value is very close to that (0.162) for complete combustion of the carbon to  $\text{CO}_2$ . This observation, of no CO being detected above the bed at  $900^\circ\text{C}$ , needs qualifying. In fact, CO was sometimes found above a bed at  $900^\circ\text{C}$ , but for values of  $\theta$  above 0.83, *i.e.* for less than 20 % excess air. Also, CO actually persisted some distance above a shallower bed (unfluidised depth  $\sim 30$  mm) at  $900^\circ\text{C}$  with  $\theta = 0.83$ . Thus the combustion of CO either within or on the very top of the bed appears to be promoted by having a hotter and deeper bed, fluidised by excess air, with  $\theta \leq 0.83$ . Otherwise, CO probably persists and burns in the freeboard.

Interestingly the temperature in the freeboard is seen in Fig. 8 to fall from 900 to  $\sim 820^\circ\text{C}$ , no doubt because of poor thermal insulation around the upper part of the tube housing the bed. Thus this drop in temperature of  $\sim 80^\circ\text{C}$  is larger than that of  $\sim 37^\circ\text{C}$  in Fig. 7 for the cooler bed, above which some combustion did liberate heat. A comparison of Figs. 7 and 8 would indicate that, if there is a minimum temperature for these gaseous fuels to burn completely within the bed, its value looks to be somewhere between 750 and  $900^\circ\text{C}$ . Interestingly, Menon *et al.* concluded recently [3] that the threshold temperature for total burning of glycerol inside a bed was  $\approx 800^\circ\text{C}$ . That estimate appears to be not far off the mark.

#### 4. Conclusions

This study has shown that, when this fluidised bed burning glycerol was operated very fuel-lean ( $\theta < 0.7$ ) at  $700 - 900^\circ\text{C}$ , in effect no CO was detected well downstream above the bed. In fact, all the carbon in the glycerol then appeared quantitatively as  $\text{CO}_2$ . What is happening? It was recognised above that this way of burning glycerol, by injecting it into the bottom of a hot bed, gives bubbles of glycerol vapour at the bottom of the bed. These bubbles meander sideways and rise up the bed, surrounded by bubbles of fluidising air. Because the bed is at least at  $700^\circ\text{C}$ , there is rapid thermal decomposition of the glycerol vapour, with the major products being mainly CO and  $\text{H}_2$ . Subsequently, these gaseous fuels have to mix with  $\text{O}_2$ , by each bubble exchanging some of its contents with the gas moving interstitially between the fluidised particles. Finally, combustion of a suitable mixture of  $\text{O}_2$  with CO,  $\text{H}_2$  or a hydrocarbon like  $\text{CH}_4$  can occur: (i) in bubbles rising up the bed, especially one hotter than  $\sim 900^\circ\text{C}$  [22, 25, 26], (ii) in the interstices between the fluidised particles, but

only for  $H_2$  [21], (iii) as a flat premixed flame sitting on the upper surface of the bed, as observed previously [27], when  $U$  only slightly exceeds  $U_{mf}$ , so there are no bubbles, (iv) in bubbles bursting and disengaging from the top of the bed [25, 26] or (v) in the freeboard [22], before the gas is sampled for analysis. The above sequence of events is complex, but one simplification is that  $H_2$  is likely to diffuse and burn readily, even between the fluidised particles, at temperatures as low as  $500^\circ\text{C}$  [21]. However, CO is a more difficult fuel to burn, particularly in a fluidised bed [11, 22]. This is partly due to the reaction:  $\text{CO} + \text{OH} \rightarrow \text{CO}_2 + \text{H}$  being relatively slow [28], but also to the radicals propagating combustion, such as OH and free atoms of O and H, recombining with one another on the huge surface area of the particles [25, 27]. This is why CO often appears well downstream in the off-gas from a bed burning more fuel-rich mixtures of glycerol, *i.e* with  $\theta > 0.7$ . This was noted in Figs 3 and 4.

The main practical requirement is for complete combustion to occur within a fluidised bed and not above it [29]. This is to take advantage of heat transfer from a fluidised bed to immersed cooling tubes being significantly faster than from a hot gas to such tubes [30]. This work has identified some of the parameters affecting the combustion of glycerol in an electrically heated bed of alumina particles fluidised by air. Quite strikingly, varying the temperature from  $700$  to  $900^\circ\text{C}$  had little effect on the mechanism of combustion. This was attributed to the slowness, at which the products of the thermal decomposition of glycerol (mainly CO and  $H_2$ ) mixed with the air from bubbles, percolating between the particles. Of course, molecules of  $H_2$  diffuse relatively rapidly, so the problem is one of mixing  $O_2$  from bubbles of air with CO and hydrocarbons such as  $\text{CH}_4$ , formed from glycerol in separate bubbles of fuel. As for the other variables, the equivalence ratio,  $\theta$ , should be kept below a critical value for no CO to be detected above the bed, *i.e* a fuel-lean mixture is desirable. This critical value,  $\theta_{\text{crit}} = 0.7$  was measured for particles with an unfluidised depth of 162 mm,  $U/U_{mf} = 2.5$  and particles sieved from 355 – 425  $\mu\text{m}$ . Most probably  $\theta_{\text{crit}}$  depends on the size of the bubbles and therefore on  $U_{mf}$  and thus on the diameter of the fluidised particles. It was found that increasing  $(U/U_{mf})$  promotes both mixing and combustion. Using a deeper bed can lead to poorer mixing, probably because of larger bubbles being formed.

The “popping” noises, emitted especially by shallow beds at lower temperatures, were for the first time conjecturally associated with the explosive ignition of  $H_2$  in bubbles of an appreciable size. The thermal decomposition of glycerol yields  $H_2$  as a major product. There seems to be little doubt that  $H_2$  is one fuel, which can burn between the fluidised particles; thus conditions have to be special (lower temperatures and probably shallow beds) for bubbles containing  $H_2$  and  $O_2$  to form. This would suggest that the popping sounds heard, when *e.g.* a mixture of propane and air fluidises a bed [11, 13], could be caused by propane first decomposing thermally to produce  $H_2$ , rather than by bubbles of propane and  $O_2$  simply igniting explosively. Overall, this study has revealed much about how gases, such as  $H_2$ , CO and hydrocarbons, burn in a fluidised bed.

This work is being followed by a study of the combustion of industrial waste glycerol, for comparison with the present results for pure glycerol.

### **Acknowledgement**

We warmly thank Mrs Weiyao Ma for her help providing equipment, particularly the electronics, for these experiments.

### **References**

- [1] Cremonez, P. A., Feroldi, M., Nadaleti, W.C., de Rossi, E., Feiden, A., de Camargo, M.P., Cremonez, F.E., Klajn, F.F., Biodiesel production in Brazil: Current scenario and perspectives, *Renewable Sustainable Energy Revs*, 2015; 42; 415 - 428.
- [2] Quispe, C. A. G., Coronado, C. J. R., Carvalho Jr, J. A., Glycerol: production, consumption, prices, characterization and new trends in combustion, *Renewable Sustainable Energy Revs*, 2013; 27; 475 - 493.
- [3] Menon, A., Waller, N., Wenting Hu, Hayhurst, A.N., Davidson, J.F., Scott, S.A., The combustion of solid paraffin wax and of liquid glycerol in a fluidised bed, *Fuel*, 2017; 199; 447 – 455.
- [4] Stubington, J.F., Davidson, J.F., Gas-phase combustion in fluidised beds, *A.I.Ch.E., J.*, 1981; 27; 59 – 65.
- [5] Bohon, M.D., Metzger, B.A., Linak, W.P., King, C.J., Roberts, W.L., Glycerol combustion and emissions, *Proc. Combust. Inst.*, 2011; 33; 2717 – 2724.

- [6] Steinmetz, S.A., Herrington, J.S., Winterrowd, C.K., Roberts, W.L., Wendt, J.O.L., Linak, W.P., Crude glycerol combustion: particulate, acrolein, and other volatile organic emissions, *Proc. Combust. Inst.*, 2013; 34; 2749 – 2757.
- [7] Metzger, B., Glycerol combustion, M.Sc. Thesis, N. Carolina State University, Raleigh, 2007.
- [8] Gupta, M., Kumar, N., Scope and opportunities of using glycerol as an energy source, *Renewable Sustainable Energy Revs*, 2012; 16; 4551 – 456.
- [9] Gibson, I.A., Slim, C.J., Yaoyao Zheng, Scott, S.A., Davidson, J.F., Hayhurst, A.N., An examination of Wen and Yu's formula for predicting the onset of fluidisation, *Chem. Eng. Res. Des.*, 2018; 135; 103 – 111.
- [10] Pemberton, S.T., Davidson, J.F., Turbulence in the freeboard of a gas-fluidised bed; the significance of ghost bubbles, *Chem. Eng. Sci.*, 1984; 39; 829 – 840.
- [11] Hayhurst, A.N., Does carbon monoxide burn inside a fluidized bed? A new model for the combustion of coal-char particles inside a fluidized bed. *Combust. Flame*, 1991; 85; 155 – 168.
- [12] Żukowski, W., The pressure pulses generated by the combustion of natural gas in bubbling fluidized beds, *Combust. Flame*, 2002; 130; 15 – 26.
- [13] Bulewicz, E.M., Żukowski, W., Kandefer, S., Pilawska, M., Flame flashes when bubbles explode during the combustion of gaseous mixtures in a bubbling fluidised bed, *Combust. Flame*, 2002; 132; 319 – 327.
- [14] Chadeesingh, D.R., Hayhurst, A.N., *Combust. Flame*, The combustion of a fuel-rich mixture of methane and air in a bubbling fluidised bed of silica sand at 700°C and also with particles of Fe<sub>2</sub>O<sub>3</sub> or Fe present, *Fuel*, 2014; 127; 169 – 177.
- [15] Gaydon, A.G., Wolfhard, H.G., *Flames, their structure, radiation and temperature*, 4<sup>th</sup> ed., Chapman & Hall, London, 1979, pp. 11, 201.
- [16] Barker-Hemings, E., Cavallotti, C., Cuoci, A. Faravelli, T., Ranzi, E., A detailed study of pyrolysis and oxidation of glycerol (propane-1, 2, 3-triol, 7<sup>th</sup> Medit., *Combust. Symp.*, Cagliari, Sardinia, Sept., 2011, 12 pp.
- [17] Stein, Y.S., Antal, M.J., Jones, M., A study of the gas-phase pyrolysis of glycerol, *J. Anal. Appl. Pyrolysis*, 1983; 4; 283 – 296.

- [18] Valliyappan, T., Ferdous, D., Bakhshi, N.N., Dalai, A.K., Production of hydrogen and syngas via steam gasification of glycerol in a fixed-bed reactor, *Topics in Catalysis*, 2008; 49; 59 – 67.
- [19] Davidson, J.F., Harrison, D, *Fluidised particles*, Cambridge University Press, Cambridge, 1963, pp. 53, 95.
- [20] Clift, R., Grace, J.R., in Davidson, J.F., Harrison, D, Clift, R., *Fluidization*, 2<sup>nd</sup> Ed., Academic Press, London, 1985, pp. 76, 114.
- [21] Baron, J., Bulewicz, E.M., Kandefer, S., Pilawska, M., Żukowski, W., Hayhurst, A.N., Combustion of hydrogen in a bubbling fluidized bed, *Combust. Flame*, 2009; 156; 975 – 984.
- [22] Hayhurst, A.N., Tucker, R.F., The combustion of carbon monoxide in a two-zone fluidized bed, *Combust. Flame*, 1990; 79, 175 – 189.
- [23] Chadeesingh, D.R., Hayhurst, A.N., The combustion of mixtures of methane and air in bubbling fluidized beds of hot sand, 19<sup>th</sup> Int., Conf. Fluid Bed Combustion, Vienna, 2006, pp. 288 – 297 (ISBN 3-200-00645-5).
- [24] Darton, R.C., La Nauze, R.D., Davidson, J.F., Harrison, D., Bubble growth due to coalescence in fluidized beds, *Trans. I. Chem. Eng.*, 1977; 55; 274 – 280.
- [25] Dennis, J.S., Hayhurst, A.N., Mackley, I.G., The ignition and combustion of propane/air mixtures in a fluidised bed, *Proc. Combust. Inst.*, 1982; 19; 1205 – 1212.
- [26] Hayhurst, A.N., John, J.J., Wazacz, R.J., The combustion of propane and air as catalysed by platinum in a fluidised bed of hot sand, *Proc. Combust. Inst.*, 1998; 27; 3111 – 3118.
- [27] Hesketh, R.P., Davidson, J.F., Combustion of methane and propane in an incipiently fluidized bed, *Combust. Flame*, 1991; 85; 449 – 467.
- [28] Griffiths, J.F., Barnard, J.A., *Flame and Combustion*, 3<sup>rd</sup> Ed., Chapman and Hall, London, 1995, p.106.
- [29] Miccio, M., Miccio, F., Fluidized Combustion of liquid fuels: pioneering works, past applications, today's knowledge and opportunities, *Proc. 20<sup>th</sup> Int. Conf. Fluidized Bed Combust.*, Springer, Berlin, 2009, pp. 71 – 82.
- [30] Xavier, A.M., Davidson, J.F., Heat transfer to surfaces immersed in fluidised beds, particularly tube arrays, *Fluidization*, Second Int. Conf. on Fluidization, Cambridge (Eds:

J.F. Davidson, D.L. Keairns) Cambridge University Press, Cambridge, 1978, pp. 333 – 338.

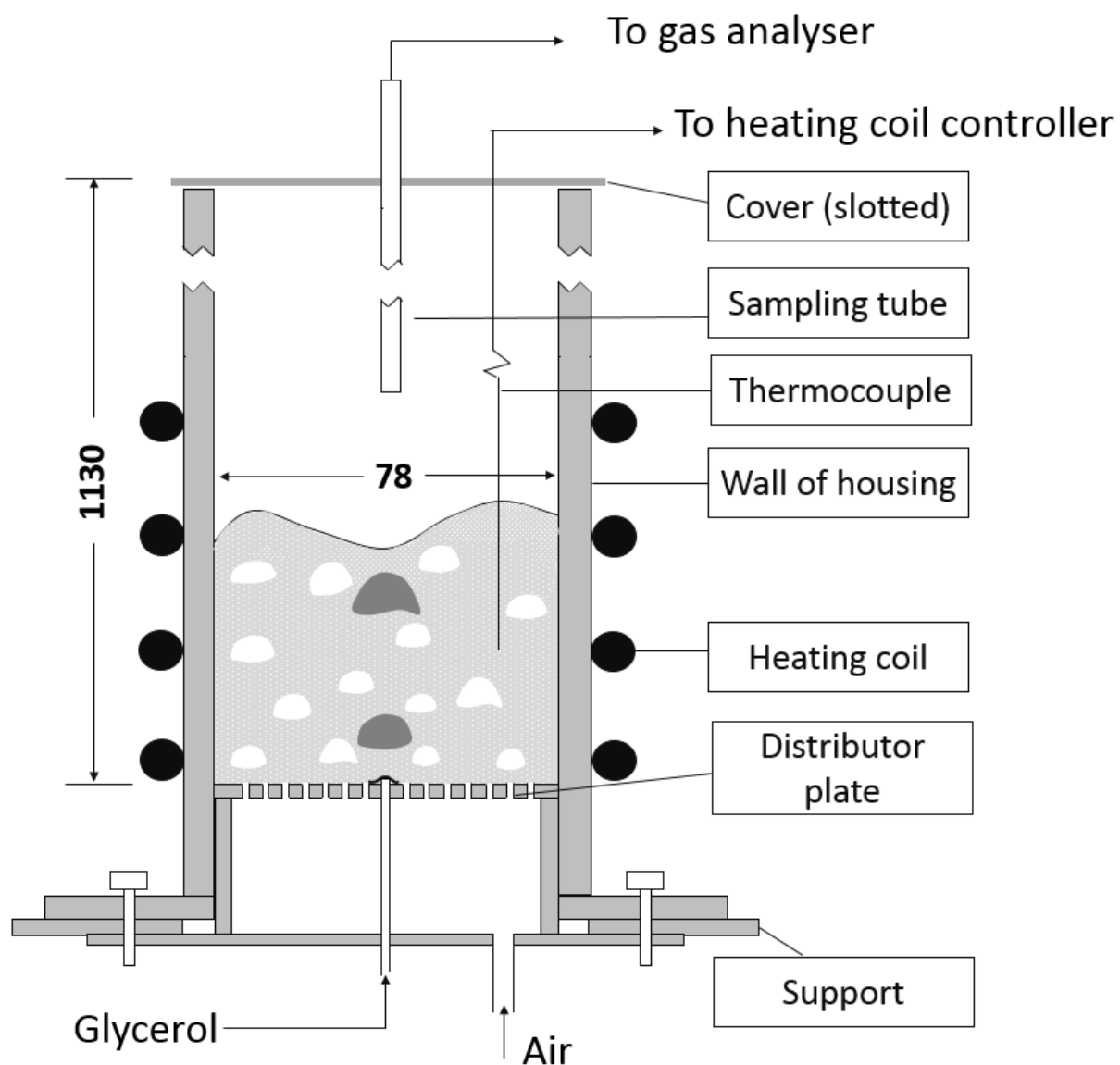


**Fig. 1.** Outline sketch (not to scale) of the electrically heated bed of alumina particles fluidised by air. Liquid glycerol was continuously pumped via a narrow tube to the centre of the distributor. The tip of the feed tube was covered by wire mesh, as shown. The tube for sampling the off-gas is also shown. Typical depths of the bed ranged from 50 to 250 mm. The central grey bubbles of glycerol vapour are surrounded by white bubbles of air. All dimensions are in mm.

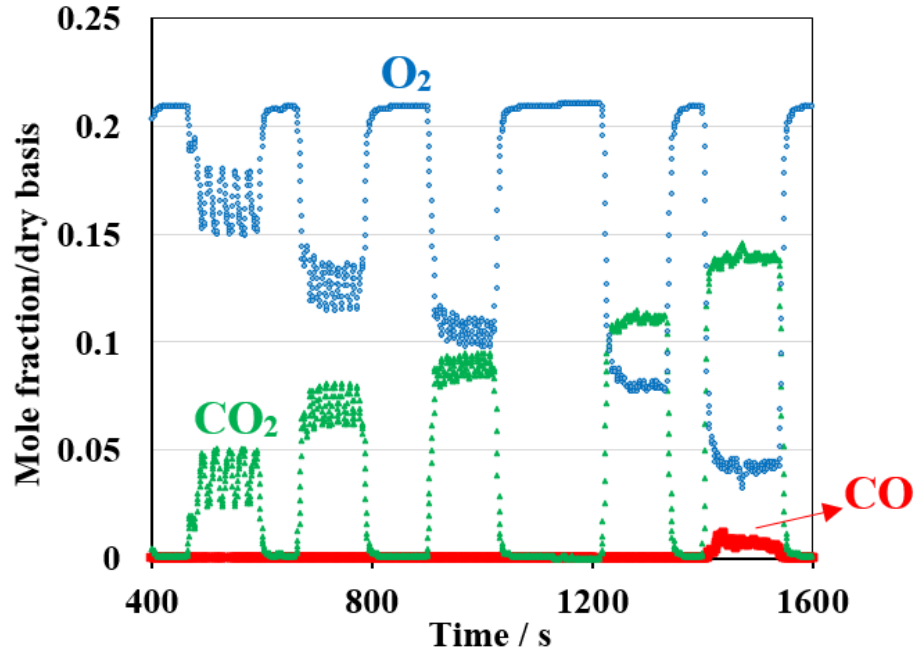


**Fig. 2.** Typical traces of the mole fractions (on a dry basis) in the off-gas from a combustion experiment. The intervals between the five, successive additions of progressively more glycerol have been truncated for clarity; the time-scale was adjusted accordingly. Each ‘peak’ for  $\text{CO}_2$  and the “trough” for  $\text{O}_2$  represent one continuous combustion run or “burn” at fixed conditions. After each ‘burn’, air was passed through the hot bed to return the conditions within the bed and sampled gas to  $x_{\text{O}_2} = 0.21$  and  $x_{\text{CO}_2} = x_{\text{CO}} = 0$ . The unfluidised depth of the bed was 162 mm, with  $U / U_{mf} = 2.5$ ,  $T_{\text{bed}} = 700^\circ\text{C}$ .



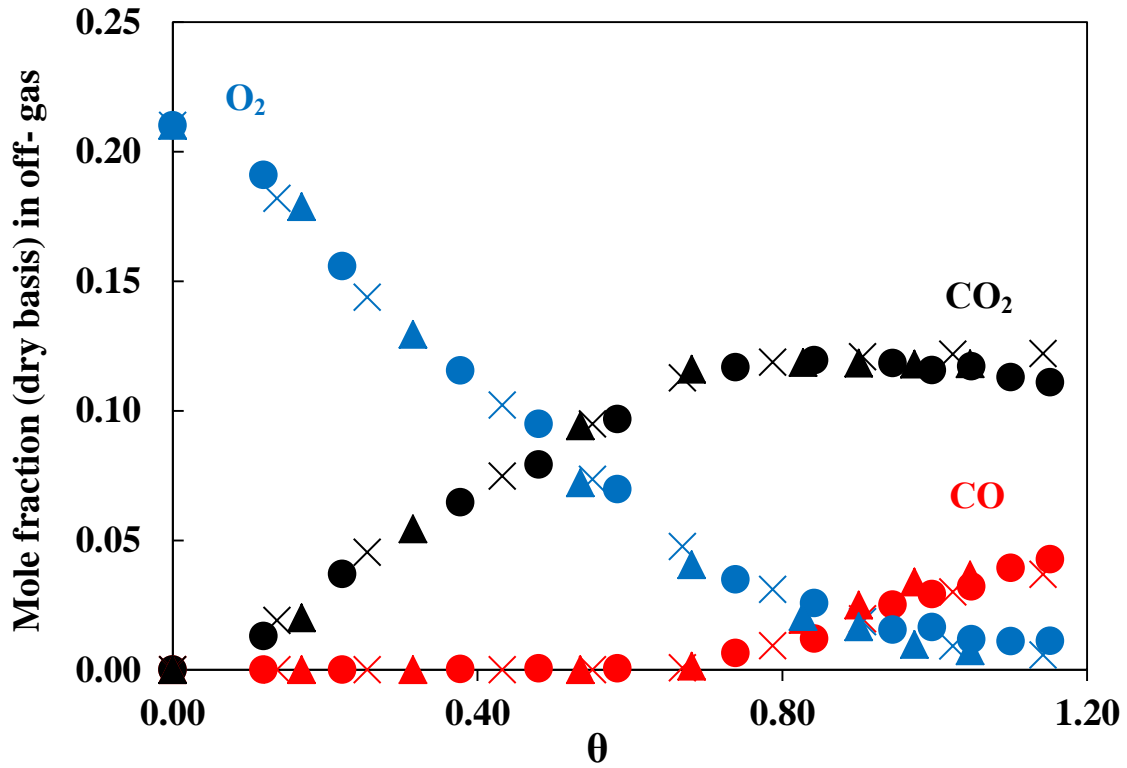


**Fig. 3.** Measured mole fractions of O<sub>2</sub> (blue), CO (red) and CO<sub>2</sub> (black) in the exhaust gas for different equivalence ratios,  $\theta$ , when burning different amounts of glycerol in air in the fluidised bed. The experiments were at :  $\bullet$  700°C,  $\times$  800°C,  $\blacktriangle$  900°C. The fluidised depth of the bed was  $\approx$  175 mm with  $(U/U_{mf}) = 2.5$ .

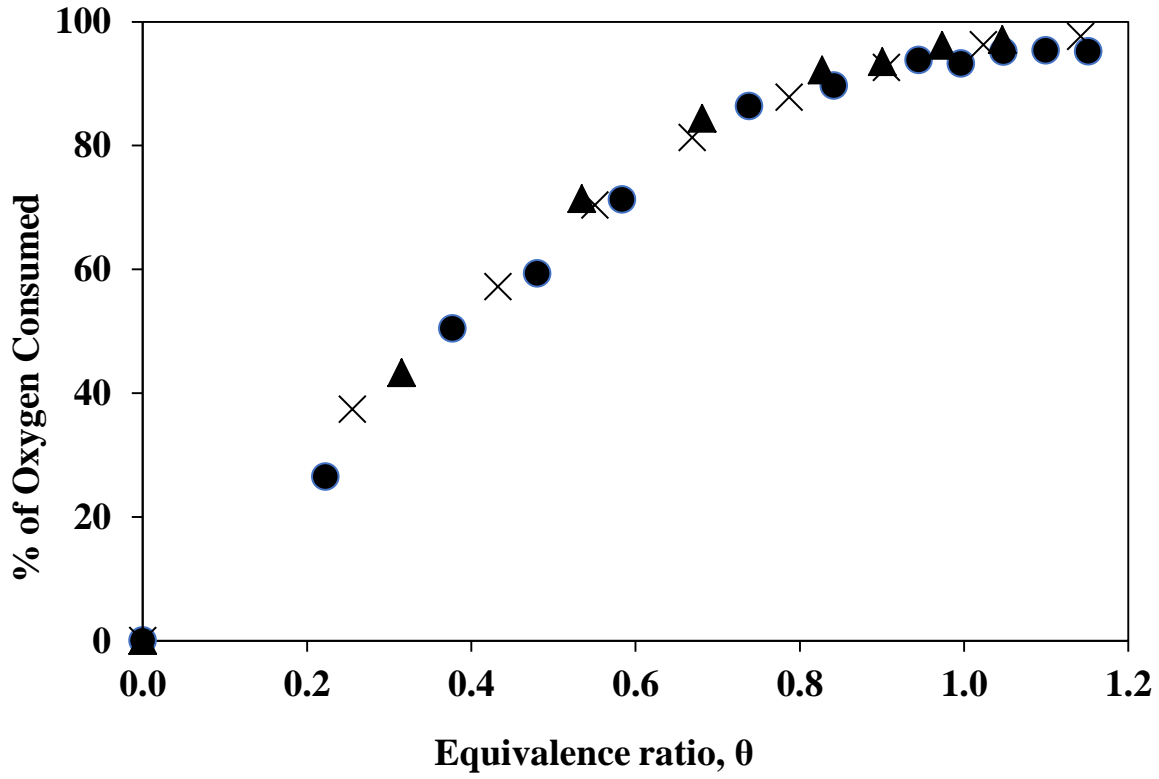


**Fig. 4.** The measured consumption of oxygen (uncertainty  $\sim 5\%$ ) for different equivalence ratios in a bed 162 mm deep, when unfluidised, with  $(U/U_{mf}) = 2.5$ . The temperatures were:  $\bullet$  700°C,  $\times$  800°C,  $\blacktriangle$  900°C.

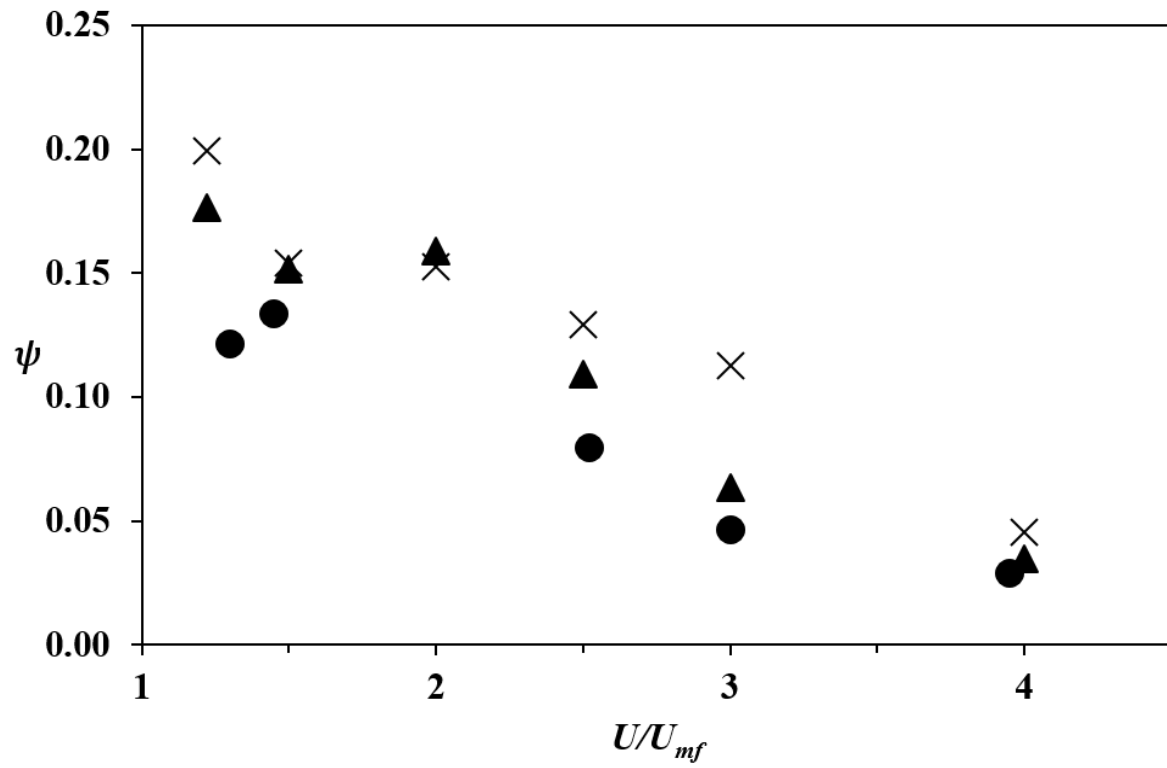


**Fig. 5.** The measured  $\psi = x_{CO} / (x_{CO} + x_{CO2})$  for different ( $U/U_{mf}$ ) and 20 % excess air for beds 162 mm deep when not fluidised. The uncertainty in  $\psi$  was  $\sim 5\%$ . The temperatures of the bed were: ● 700°C, × 800°C, ▲ 900°C.

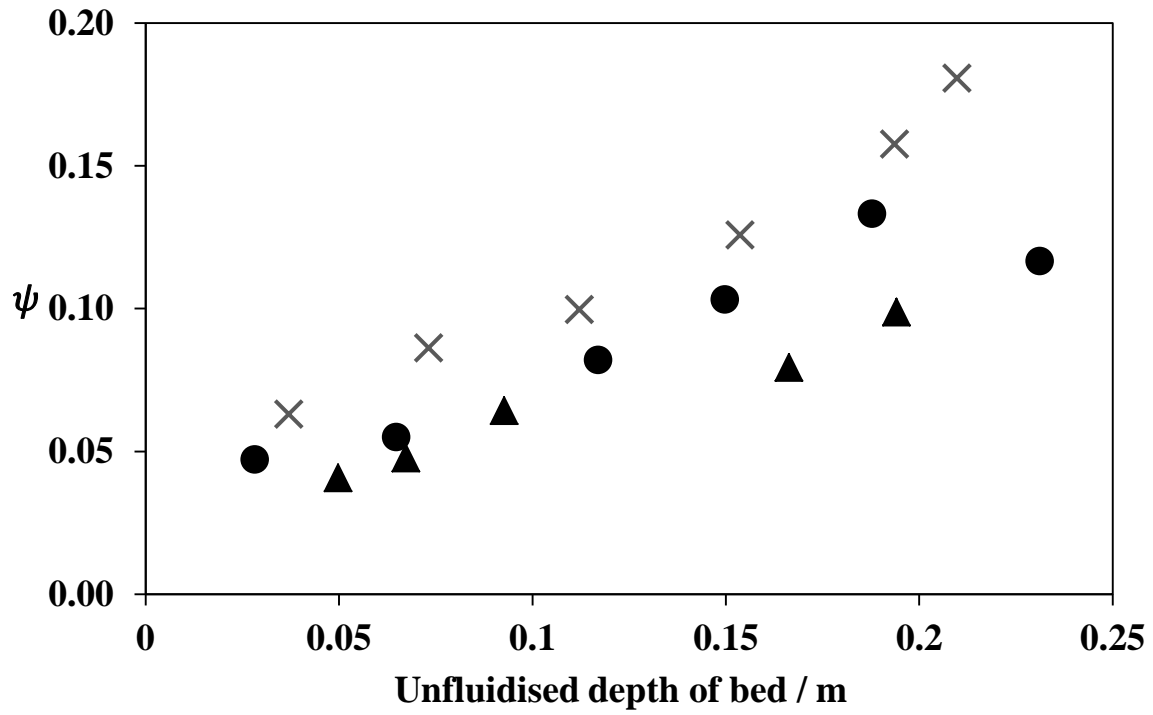


**Fig. 6.** The values of  $\psi = x_{\text{CO}} / (x_{\text{CO}} + x_{\text{CO}_2})$  measured for different depths of bed (when unfluidised) at  $\theta = 0.83$  and  $U/U_{mf} = 2.5$ . The temperatures were: ● 700°C, × 800°C, ▲ 900°C.

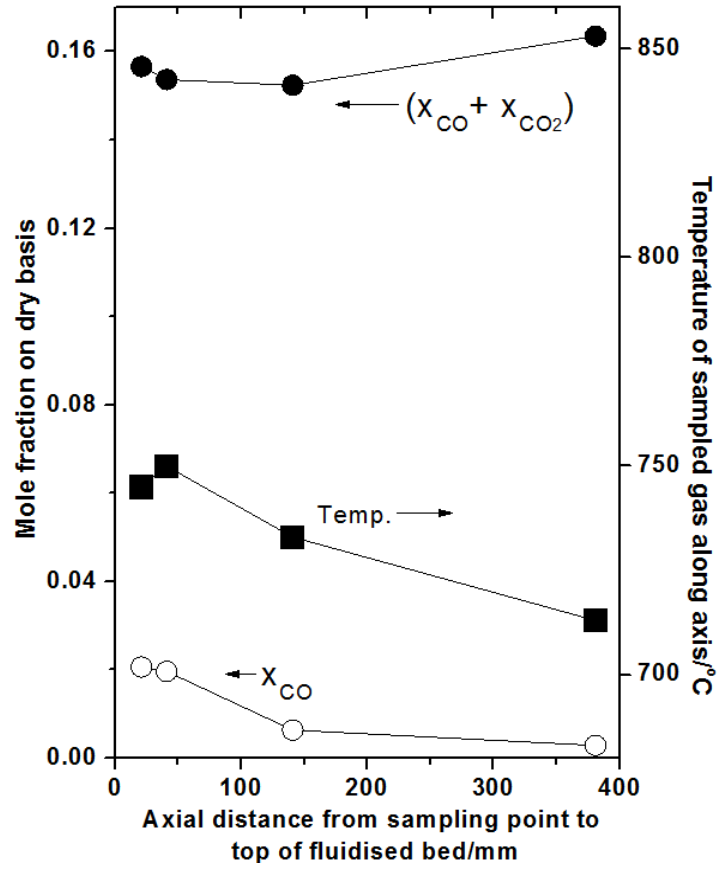


**Fig. 7.** Temperature and concentration profiles above a bed fluidised at 750°C, burning glycerol with 20% excess air ( $\theta = 0.83$ ),  $U/U_{mf} = 2.5$ , unfluidised depth of bed = 149 mm.

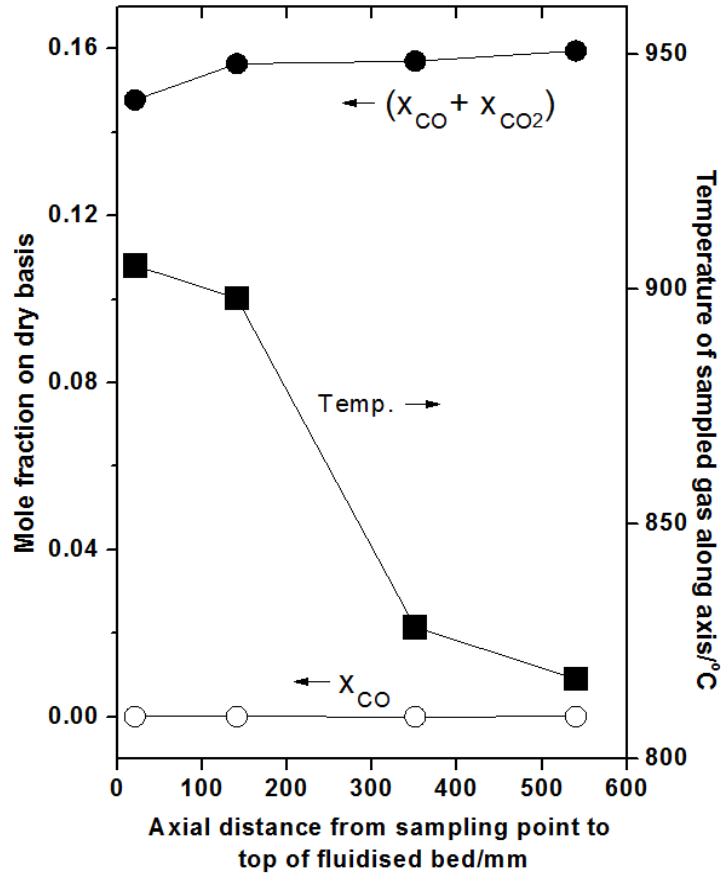


**Fig. 8.** Temperature and concentration profiles above a fluidised bed at 900°C burning glycerol with 20% excess air ( $\theta = 0.83$ ),  $U/U_{mf} = 2.5$ , unfluidised depth of bed = 149 mm.